Retreat rates, modalities and agents responsible for erosion along the coastal chalk cliffs of Upper Normandy: the contribution of terrestrial laser scanning

Pauline Letortu, Stéphane Costa, Olivier Maquaire, Christophe Delacourt, Emmanuel Augereau, Robert Davidson, Serge S. Suanez, Jean Nabucet

Retreat rates, modalities and agents responsible for erosion along the coastal chalk cliffs of Upper Normandy: the contribution of terrestrial laser scanning

Pauline Letortu[a,b*], Stéphane Costa[b], Olivier Maquaire[b], Christophe Delacourt[c], Emmanuel Augereau[c], Robert Davidson[b], Serge Suanez[a], Jean Nabucet[d]

[a]*University of Bretagne Occidentale, Laboratory LETG-Brest Géomer, IUEM, Rue Dumont d'Urville, 29280 Plouzané, France*

[b]*University of Caen Basse-Normandie, Laboratory LETG-Caen Géophen, Esplanade de la Paix, 14000 Caen, France*

[c]*University of Bretagne Occidentale, Laboratory Domaines Océaniques, IUEM, Rue Dumont d'Urville, 29280 Plouzané, France*

[d]*University of Rennes 2, Laboratory LETG-Rennes Costel, Place du Recteur Henri Le Moal, 35000 Rennes, France*

* Corresponding author. Tel.: +33 298498688; fax: +33 298498703, pauline.letortu@univ-brest.fr

Abstract:

In order to follow all the changes affecting the coastal chalk cliff face in Upper Normandy and improve knowledge about cliff erosion, repeated terrestrial laser scanning (TLS) surveys were carried out frequently between 2010 and 2013 (every 4–5 months). They were conducted at two sites with similar lithostratigraphic characteristics but different exposures to marine actions (the former being an abandoned cliff and the latter an active cliff). They provide a quantification of the production of debris with centimeter precision (from ± 0.01 to 0.04 m). These surveys provided three major outcomes: 1) cliff retreat rates were measured at high spatial resolution with retreat values, unsurprisingly, 3-4 times higher for an active cliff than for an abandoned cliff. This result highlights that marine actions should be seen as not only a transport agent but also a particularly effective erosion agent; 2) a significant

proportion of debris fall production (about 25%) in the total active cliff retreat was identified; and 3) one of the modalities of retreat was visualized as the creation of a basal notch, which propagates instability towards the upper part of the cliff face. Later, this instability generates rock falls coming from the whole cliff face.

Highlights:

- Two sites with similar lithology but different exposures to marine actions are studied.
- Cliff face changes over time and by location are examined using TLS.
- Marine actions are an effective agent of erosion.
- The proportion of debris fall production is about 25% in the active cliff retreat.
- A basal notch propagates instability towards the upper part of the cliff face.

Keywords: Coastal chalk cliff; Retreat rates; Retreat modalities; Agents for erosion; Terrestrial laser scanning; Upper Normandy

1. Introduction

To understand the regressive dynamics of coastal cliffs, the knowledge of retreat rates at fine scale and the study of agents leading to erosion are major challenges (Trenhaile, 1987; Sunamura, 1992; Griggs and Trenhaile, 1994; Stephenson et al., 2013). Erosion is traditionally quantified by studying the rates of retreat of a spatial object tracked over time, often the cliff top (Bird, 2008). However, these average retreat rates are incomplete information because they do not reflect the sudden nature of the hazard. This results in rock falls that threaten populations located at the cliff top and at the cliff foot. Thus, retreat occurs in “jerks”, generated by the interaction of both internal factors (e.g., rock strength and structure) and external factors (e.g., rainfall, temperature variations, and wave action). The contribution of the latter to triggering rock falls is difficult to determine (Letortu et al., in press). “Rock fall” is used in this paper to describe movements of coherent rock (Varnes, 1978). From Varnes’ typology, two types of movement can be distinguished according to the

fallen volume: 1) debris falls describe the small-scale release of tiny blocks or flakes (up to decimeter) from across the cliff face; and 2) rock falls describe large-scale movements from all or part of the cliff face. The former are common on rocky slopes but are often omitted in quantification due to their fine scale or unsuitable point of view. Far from negligible, their participation is estimated at about 10% of the total retreat (May and Heeps, 1985; Hénaff et al., 2002) and may be an early sign of instability. Monitoring these jerks requires a high spatial and temporal resolution and a horizontal point of view that enables all changes to be monitored (Young et al., 2009).

Due to unstable and subvertical cliff faces, quantification is difficult and sometimes dangerous. For these reasons, remote sensing technologies are mainly used. Aerial images can be used but the data accuracy is, at best, pluridecimeter and the point of view is inappropriate (vertical or oblique). Recent advances in remote sensing technology, in particular the improvement in the spatial resolution, may provide effective measurement tools. They may also offer the opportunity of conducting surveys at higher temporal frequency. Satellite data are interesting but their spatial resolution still appears insufficient for monitoring debris falls. Photogrammetry is not used because its reliability is affected by the height of the cliffs (Lim et al., 2005) but new developments are promising. Terrestrial Laser Scanning (TLS) is particularly convenient because the temporal and spatial resolution, as well as the point of view, can be defined by the user.

The TLS technique, described as "*one of the most promising surveying techniques for rockslope characterization and monitoring*" (Abellán et al., 2009), has been widely used in the study of mass transfers to:

1) identify structural and geomorphological characteristics of landslides (Oppikofer et al., 2009; Sturzenegger and Stead, 2009; Rothmund et al., 2013), landslide mapping (Rowlands et al., 2003) and displacement tracking (Delacourt et al., 2007; Oppikofer et al., 2008, 2012; Teza et al., 2008; Travelletti et al., 2008, 2013; Abellán et al., 2009, 2010);

2) analyze rock falls including those affecting cliffs (Lim et al., 2005, 2010; Rosser et al., 2005, 2013; Quinn et al., 2010; Dewez et al., 2013; Abellán et al., 2014; Kuhn and Prüfer, 2014);

3) analyze warning movements of falls (Rosser et al., 2007; Abellán et al., 2009, 2010; Royán et al., 2014).

In our study, TLS is used for repeated surveys in order to observe the evolution of the cliff face at two sites with a similar lithological context but subject to different marine forcing (abandoned and active cliffs). The aim is to quantify erosion at fine scale, to visualize the modalities of retreat and to contribute to the debate about the agents responsible for erosion of the Upper Normandy chalk cliffs. This paper first explains the study area and details the material and the TLS survey methodology. Then, the results of the cliff face monitoring are described and discussed.

2. Study area

2.1. Regional setting

Upper Normandy is located in the northwestern part of France, on both sides of the 50th northern parallel, along the English Channel (epicontinental sea, 86 m deep on average). The environment is macrotidal with a tidal range of 8 m. Swell is limited but the wind sea can reach a significant wave height of 4 m in Dieppe (annual return period). Upper Normandy has a marine west coast climate. From Météo-France data (1971–2000), average winter temperatures are positive but an average of 26 daily freeze/thaw cycles is recorded per year (minimal temperature can reach −15°C). Rainfall is distributed over the year (≈800 mm) although fall and winter are the wettest seasons (51 mm in August and 94 mm in November). Daily rainfall can exceed 77 mm in October. The Upper Normandy cliffs, 60–70 m high on average, extend 120 km from Le Havre (SW) to Le Tréport (NE) (Seine-Maritime) (Fig. 1). At their foot, there is a marine erosion platform (from 150 to 350 m wide), hidden, at the upper part of the beach, by a thin gravel beach. The cliffs are intersected by numerous drained or

dry valleys perpendicular to the coast, protected at their outlet by often wide (from 30 to 100 m) gravel beaches due to the presence of groins or harbor jetties.

At the northwestern end of the sedimentary Paris Basin and in contact with the English Channel, the Upper Normandy cliffs between Cap d'Antifer and Le Tréport are made of chalk with flints, dated as Upper Cretaceous (Pomerol et al., 1987; Mortimore and Duperret, 2004). On this highly karstified frame (Rodet, 1991), there are residual flint formations and Quaternary loess (Lautridou, 1985). The main tectonic deformations (NW–SE) have led to the outcrop of various Upper Cretaceous geological strata (Fig. 1). The different stages of chalk have slight variations in facies and fine sedimentary discontinuities, which generate some subtle resistance contrasts (Juignet and Breton, 1992; Laignel, 1997; Lasseur, 2007). From the oldest to the newest, Cenomanian chalk outcrops a few meters at the base of the cliffs of Cap d'Antifer and Etretat, and east of Fécamp. It is heterogeneous, sometimes rich in detrital components (clay and quartz), and may be glauconitic or nodular. Turonian chalk is the overlying strata. It is composed of clayish, grayish to whitish chalk, with frequent nodular beds and little or no flint. This stage outcrops from Cap d'Antifer to Etretat, from Fécamp to Eletot, and from Puys (east of Dieppe) to Le Tréport. Turonian chalk is covered with Coniacian chalk, outcropping between Cap d'Antifer and Saint-Valéry-en-Caux, and between Dieppe and Le Tréport. The overlying stage, Santonian chalk, appears in the central part of the study area between Saint-Valéry-en-Caux and Puys. Finally, Campanian chalk, the most recent one, is only found between Quiberville and Pourville-sur-Mer (Hautot-sur-Mer). In relation to geotechnical studies, Santonian and Campanian chalk seem more favorable to weathering than other stages of the Upper Cretaceous (Laignel, 1997). Over these chalk strata, a bed of clay and sand sediments about 10 to 30 m thick of Paleogene age (Bignot, 1962) replaces the usual residual flint formation (Laignel, 1997; Costa et al., 2006a), especially in Sainte-Marguerite-sur-Mer, Varengeville-sur-Mer (these two towns are located along Cap d'Ailly) and Sotteville-sur-Mer (Fig. 1).

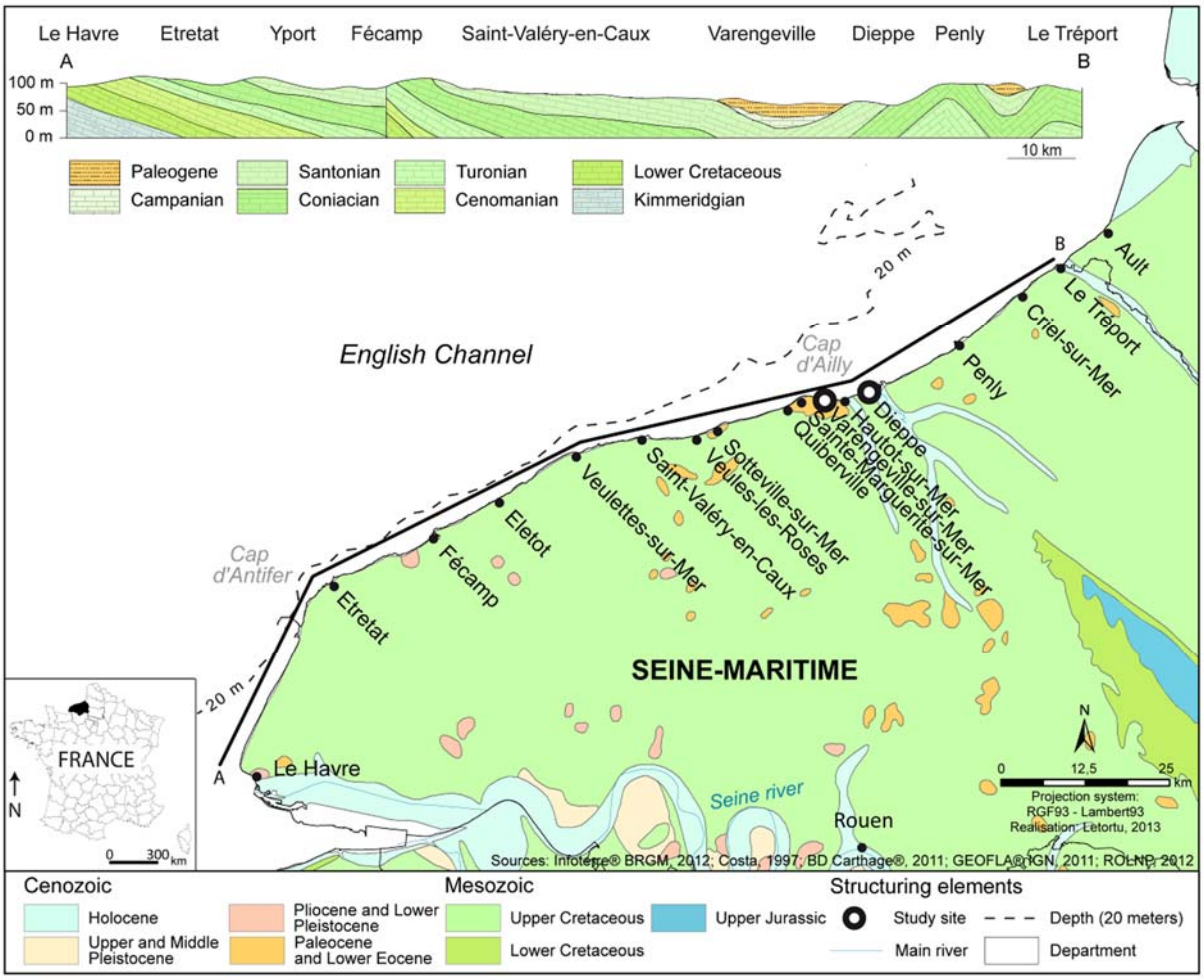

Fig. 1: Presentation of the study area

The regressive dynamics of the Upper Normandy cliffs are expressed by instantaneous rock falls affecting all or part of the cliff. At the foot of the slopes, a fine gravel beach develops but the deposits are only a few meters thick. The tracking and distribution of these beaches are affected by rock falls and man-made structures (harbor jetties and groins), which are obstacles to longshore drift. The absence of a beach or a reduced amount of beach sediments at the cliff foot may alter the effectiveness of marine actions, and therefore the intensity and modalities of erosion (Costa et al., 2006b).

The regressive dynamics followed by the cliff top between 1966 and 2008 (photogrammetry and orthophotography) reveal a retreat rate of 0.15 m y^{-1} with high spatial variability in Upper Normandy (Costa et al., 2004; Letortu, 2013; Letortu et al., 2014). However, these average retreat rates provide only fragmentary information because they do not describe the sudden

nature of the departure of material. For example, on 19 December 2012 in Dieppe, a rock fall of approximately 100,000 m^3 resulted in a cliff top retreat of 40 m in a few seconds while the average annual retreat rate on this site is 0.21 m y^{-1} (Letortu et al., 2014; Michoud et al., 2014).

2.2. Site selection

To decipher the relative contribution of marine and subaerial agents in the erosion rates, two neighboring sites with similar lithological contexts (cliff made up of Coniacian and Santonian chalk) but subject to different marine forcing were selected (Figs. 1 and 2). One site is an abandoned cliff only affected by subaerial agents; the other site is an active cliff, which is evolving under the influence of both subaerial and marine agents. The abandoned cliff face is located in Dieppe. This site was divided into two areas with different cliff face orientations: one corresponding to an exposure of 280°N (named Dieppe 1 W, 45 m long, 30 m high); and the other corresponding to an exposure of 010°N (named Dieppe 2 N, 80 m long, 30 m high). The site characterized by an active cliff face is along Cap d'Ailly. More precisely, it lies on either side of the Petit Ailly dry valley in Varengeville-sur-Mer (exposure of 010°N, 250 m linear, maximum height of 40 m) (Fig. 2).

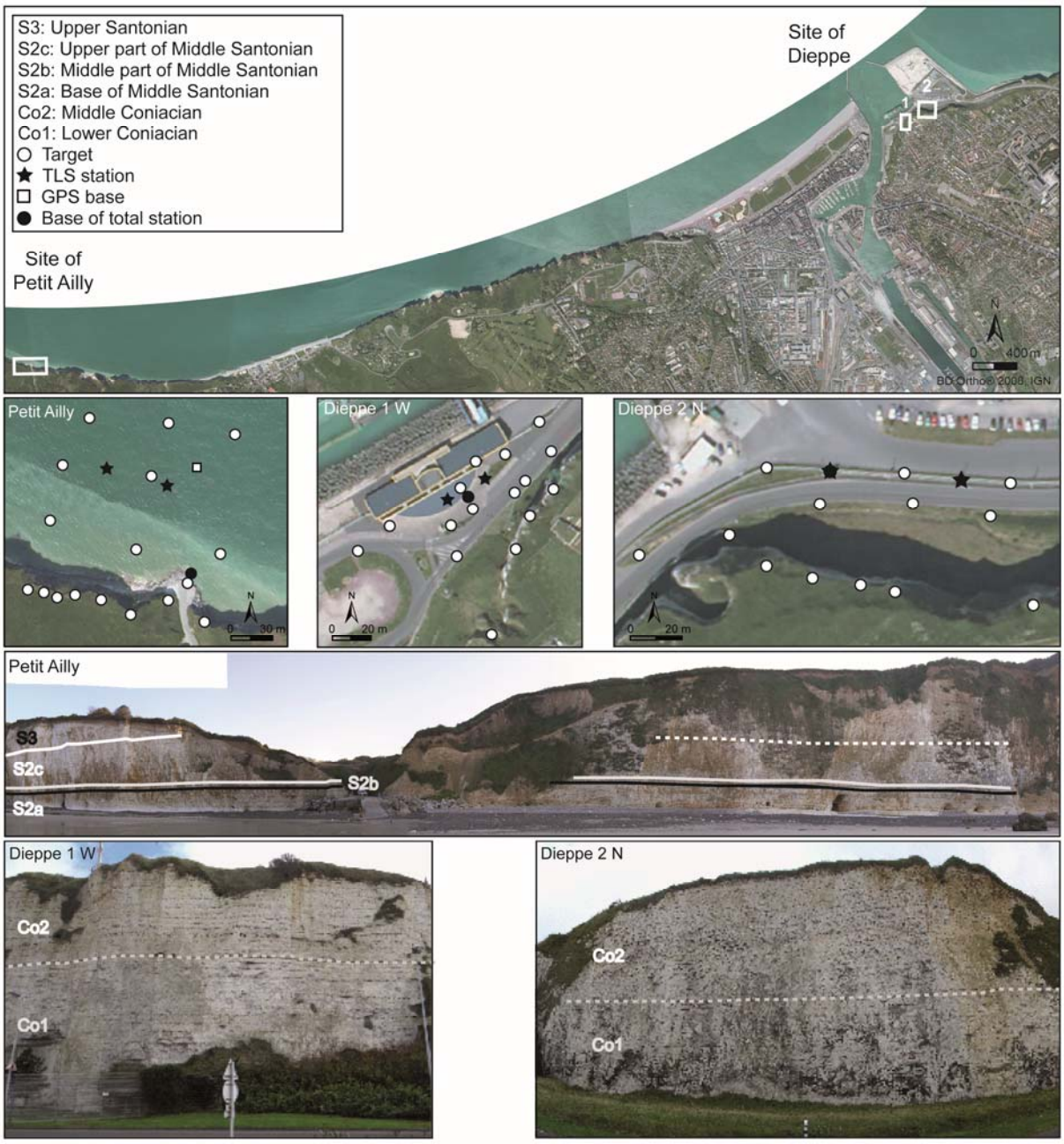

Fig. 2: Location, lithostratigraphy and panorama of Petit Ailly *and* Dieppe (1 W and 2 N)

3. Material and methods

3.1. TLS surveys

Terrestrial laser scanner is a measuring instrument that uses pulse laser technology to determine the distance from the device to the point to be measured. This distance is based on a non-contact and reflectorless acquisition of a point cloud and is measured by the time between the transmission of an infrared laser pulse and the return of the reflected pulse. The

instrument used in this study is a RIEGL LMS-Z390i emitting a wavelength of 1,550 nm, which records a single time-of-flight without any access to the complete signal form (full waveform). The theoretical range of this device is 400 m for an 80% reflective surface and 140 m for a 10% reflective surface (RIEGL, 2007).

This technique is subject to use restrictions of two types: geometric and radiometric. Regarding the geometric limitations, Lichti (2007) demonstrated the influence of the incidence angle on the measurement accuracy. This method is also affected by radiometric limitations including environmental ones. The accuracy and resolution of the scan depend on the reflection of the scanned material and the atmospheric water content. During our surveys, meteorological conditions were often good: no rainfalls, clear visibility and low wind. A discussion on the principles of TLS and its performance is provided by Teza et al. (2007). The main parameter that controls the spatial resolution is the distance between the measured point and the TLS device. The area near the TLS device has a high spatial resolution (millimeter). The distance to the scanned object is dependent on the length of the coast being monitored and its height (the vertical swath of TLS is only 80°).

During repeated surveys at these two sites, 19 point clouds were acquired over 28 months (between 10/07/2010 and 02/12/2013), every 4–5 months (Fig. 3).

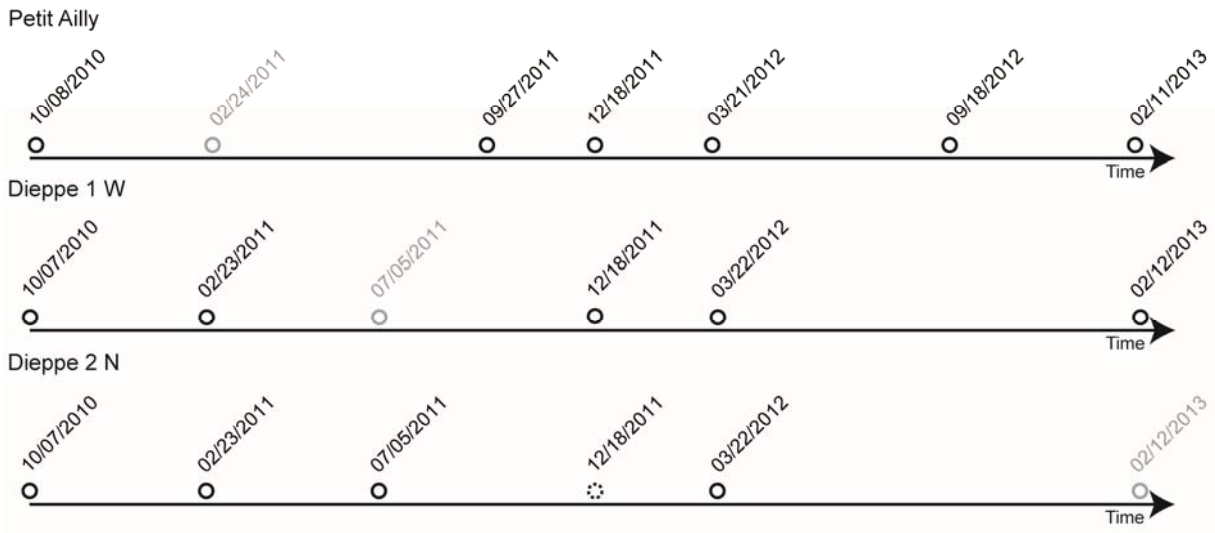

Fig. 3: Temporal distribution of point clouds between 10/07/2010 and 02/12/2013 (gray: point clouds affected by a high error margin; dotted line: unusable point cloud)

The TLS station is 33 m from the abandoned cliff of Dieppe 1 W and 37 m from Dieppe 2 N. For Petit Ailly, the TLS station is positioned at 80 m. For repeated surveys of high accuracy, the process of data acquisition requires additional equipment (Fig. 2): targets, a total station (TPS400 Leica TC410C) and a DGPS (Trimble with a base station 5,700 and a mobile receiver 5,800). The total station, where the point of setup is previously known by DGPS measurements, can replace the point cloud acquired in a relative coordinate system in an absolute coordinate system (Lambert 93 and associated RGF93 and IGN69). Although the TLS instrumental precision is ± 0.003 m to 50 m, the main source of error in data processing comes from the georeferencing of the point cloud in an absolute coordinate system via the targets (Jaud, 2011). The use of a large number of targets (16 at Dieppe 1 W, 13 at Dieppe 2 N, 17 at Petit Ailly) and the maximizing of their distance from the TLS, as long as they all remain visible, reduce the alignment error of the point cloud.

3.2. Data processing

The main steps in the data processing are 1) georeferencing and point cloud assembly; 2) point cloud cleaning; 3) meshing and interpolation to produce a Digital Elevation Model (DEM); and 4) creation of a DEM of Difference (DoD) (Jaud, 2011). Retreat is calculated by dividing the volume of change on the cliff face by the monitored area. The volume of change does not include debris material after failure because this is generally quickly removed (in a few days or weeks) at Petit Ailly, and quickly covered by vegetation at Dieppe. The retreat is then divided by years to obtain the annual retreat rate.

Of the 19 point clouds acquired, one was unusable (12/18/2011 at Dieppe 2 N) (Fig. 3, dotted line). Observation of the point cloud highlighted artifacts including the rain, which absorbed the laser pulse. Three other point clouds did not have good georeferencing (error from 0.04 to 0.08 m). Two point clouds (07/05/2011 at Dieppe 1 W and 02/12/2013 at Dieppe

225 2 N) were certainly disturbed during acquisition as a docking cross-Channel ferry created
226 significant temporary vibrations. The other one (02/24/2011 at Petit Ailly) was probably
227 disturbed by depression of the TLS during acquisition on a wet sandy foreshore. These three
228 point clouds were not used to quantify the rate of retreat, but only to study the spatial
229 distribution of material departures (Fig. 3, dates in gray). In February 2013, human activities
230 (clearing work and setup of safety nets) disturbed measurements in Dieppe. All human
231 impacts were removed in the calculations and tables to monitor the "natural" evolution of the
232 chalk cliff in Dieppe.
233
234 *3.3. Error margin*
235 To quantify the error between the DEM, fixed areas were selected, such as urban furniture in
236 Dieppe or groin at Petit Ailly in each original point cloud (just after georeferencing, step 1
237 previously described). These fixed areas are equivalent to approximately 7,000 points. These
238 data were processed with the same methodology previously mentioned in order to obtain a
239 DEM about fixed areas at each site. The final DoD revealed the margin of error of
240 measurement. The lowest margin of error was ± 0.01 m in Dieppe 2 N. At Petit Ailly, the
241 accuracy was ± 0.03 m. In Dieppe 1 W, it was ± 0.04 m. These differences were mainly due
242 to the quality of topometric data. The greatest difference was located in Dieppe 1 W because
243 topometric measurements were temporarily disturbed by a docking cross-Channel ferry and
244 renovation of the passenger terminal (building visible in Fig. 2).
245
246 **4. Results**
247 *4.1. Retreat rates and spatial distribution of erosion*
248 During the repeated surveys, in Petit Ailly, the total retreat of the cliff face was 0.57 m (± 0.03
249 m), corresponding to an annual retreat rate of 0.24 m y^{-1}. Dieppe 1 W receded by 0.08 m y^{-1}
250 while Dieppe 2 N receded by 0.06 m y^{-1} (Fig. 4). Between both orientations of Dieppe, the
251 retreat rate differences are within the margin of error. These first results highlight that the site
252 of Petit Ailly had a more intense retreat than Dieppe (0.24 m y^{-1} against 0.06–0.08 m y^{-1}),

253 marked by sudden accelerations (up to 1.16 m y^{-1} for the DoD F, Fig. 4). Unsurprisingly,
254 abandoned cliffs receded more slowly than active cliffs (3–4 times slower). This difference
255 confirms the strong influence of marine actions on the regressive dynamics of the chalk cliffs.
256 For both sites, the retreat rates were higher for the period including all or part of winter than
257 other seasons. For example, in Petit Ailly during winter 2011/2012, the retreat rate was 0.17
258 m y^{-1} while during spring and summer 2012, it was 0.06 m y^{-1}.
259 TLS surveys provide a fine location of erosion – the cliff foot corresponds to the first third of
260 the cliff height and the cliff top is the rest. The cliff top receded faster than the cliff foot, at
261 both cliffs, the active (Petit Ailly) and the abandoned ones (Dieppe): 1) 0.25 m y^{-1} at the cliff
262 top against 0.21 m y^{-1} at the cliff foot at Petit Ailly; and 2) 0.07–0.10 m y^{-1} at the cliff top
263 against 0.02–0.03 m y^{-1} at the cliff foot in Dieppe (Fig. 4).
264

Petit Ailly in the context of an active cliff (error margin: ± 0.03 m)

Previous DEM	Next DEM	Time gap (month)	Name of DoD	Retreat rate (m y^{-1})	
10/08/2010	02/24/2011	4.5	A	0.00	
02/24/2011	09/27/2011	7.0	B	0.09	
09/27/2011	12/18/2011	3.0	C	0.00	
12/18/2011	03/21/2012	3.0	D	0.17	
03/21/2012	09/18/2012	6.0	E	0.06	
09/18/2012	02/11/2013	4.5	F	1.16	
10/08/2010	02/11/2013	28.0	Total	0.24	*Cliff top erosion: 0.25 m y^{-1}* *Cliff foot erosion: 0.21 m y^{-1}*

Dieppe 1 W in the context of an abandoned cliff (error margin: ± 0.04 m)

Previous DEM	Next DEM	Time gap (month)	Name of DoD	Retreat rate (m y^{-1})	
10/07/2010	02/23/2011	4.5	A	0.07	
02/23/2011	07/05/2011	4.5	B	0.06	
07/05/2011	12/18/2011	5.5	C	0.03	
12/18/2011	03/22/2012	3.0	D	0.24	*Setup of safety net disturbing measurements*
03/22/2012	02/12/2013	10.5	E	-	
10/07/2010	03/22/2012	17.5	Total	0.08	*Cliff top erosion: 0.10 m y^{-1}* *Cliff foot erosion: 0.03 m y^{-1}*

Dieppe 2 N in the context of an abandoned cliff (error margin: ± 0.01 m)

Previous DEM	Next DEM	Time gap (month)	Name of DoD	Retreat rate (m y^{-1})	
10/07/2010	02/23/2011	4.5	A	0.10	
02/23/2011	07/05/2011	4.5	B	0.00	
07/05/2010	12/18/2011	6.5	C		
07/05/2011	03/22/2012	8.5	D	0.04	*Setup of safety net disturbing measurements*
03/22/2012	02/12/2013	10.5	E	-	
10/07/2010	03/22/2012	17.5	Total	0.06	*Cliff top erosion: 0.07 m y^{-1}* *Cliff foot erosion: 0.02 m y^{-1}*

Fig. 4: Successive retreat rates as a function of DoD (gray DEM: affected by a high error margin)

4.2. Proportion of rock falls and debris falls in the retreat

Understanding the evolution of cliff faces depends on the frequency of surveys and the erosive dynamics of cliffs. Their frequency (every 4–5 months) does not ensure that a starting area that appears homogeneous in the DoD is the result of a single rock fall.

Successive rock falls may be located at the same place. However, these different dynamics could be determined thanks to an inventory of falls collected weekly by the non-profit organization ESTRAN on the coastline studied (Letortu et al., 2014, in press). Due to the centimeter accuracy of the data and the high spatial resolution of the TLS, it is possible to separate debris falls (Fig. 5, photographs a and b) and rock falls (Fig. 5, photographs D and F).

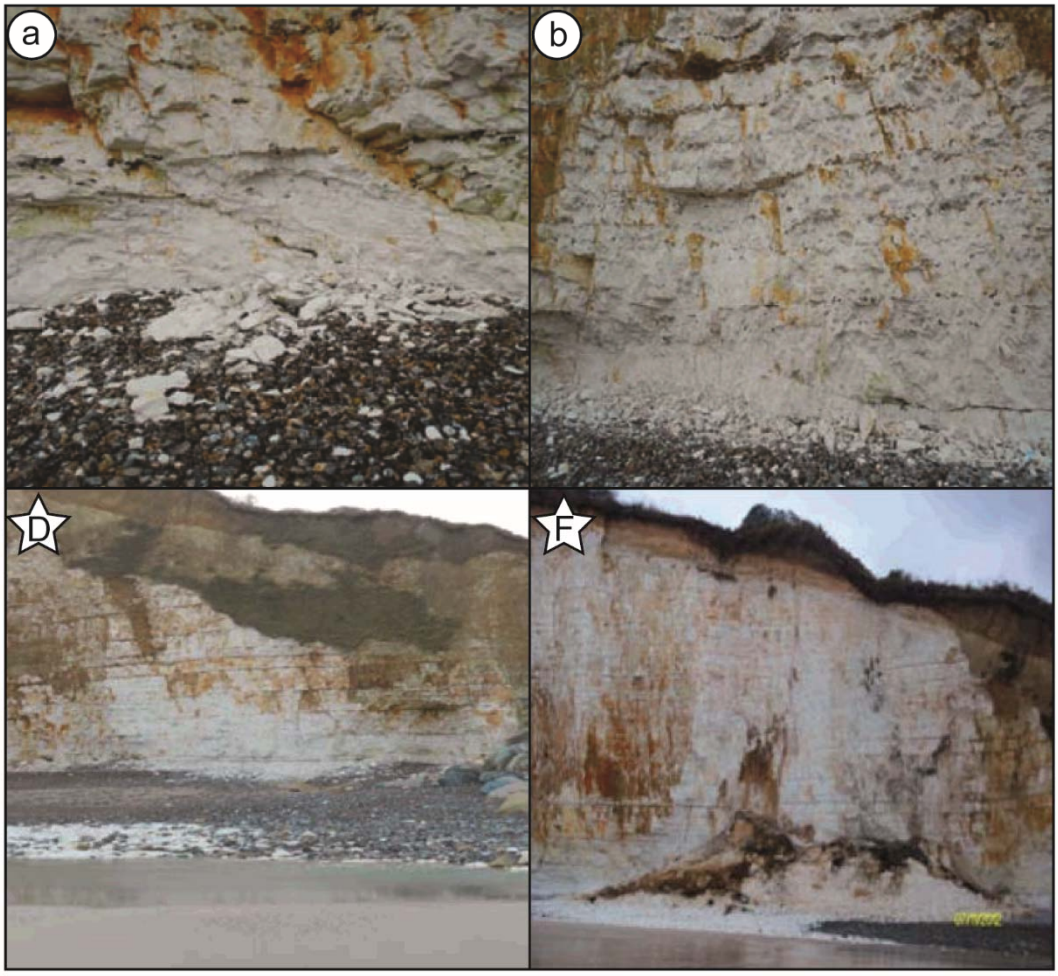

Fig. 5: Examples of debris falls (circles a and b) and rock falls (stars D and F) at Petit Ailly identified by TLS in Fig. 8 (ESTRAN organization, 2012)

Over the period studied (October 2010–February 2013), the abandoned cliff was only affected by debris falls (blue in electronic version of Figs. 6 and 7). The active cliff was affected by debris falls (dark blue in electronic version of Fig. 8) and rock falls (from light blue

to red in electronic version of Fig. 8). Rock falls (10 cases were identified from 10 to 1,636 m^3) generated local significant retreats, especially on the eastern cliff face (up to 4.71 m deep). However, the largest ones (1,636 m^3 for rock fall F and 194 m^3 for rock fall G) were observed on the DoD F between 09/18/2012 and 02/11/2013 (Fig. 8).

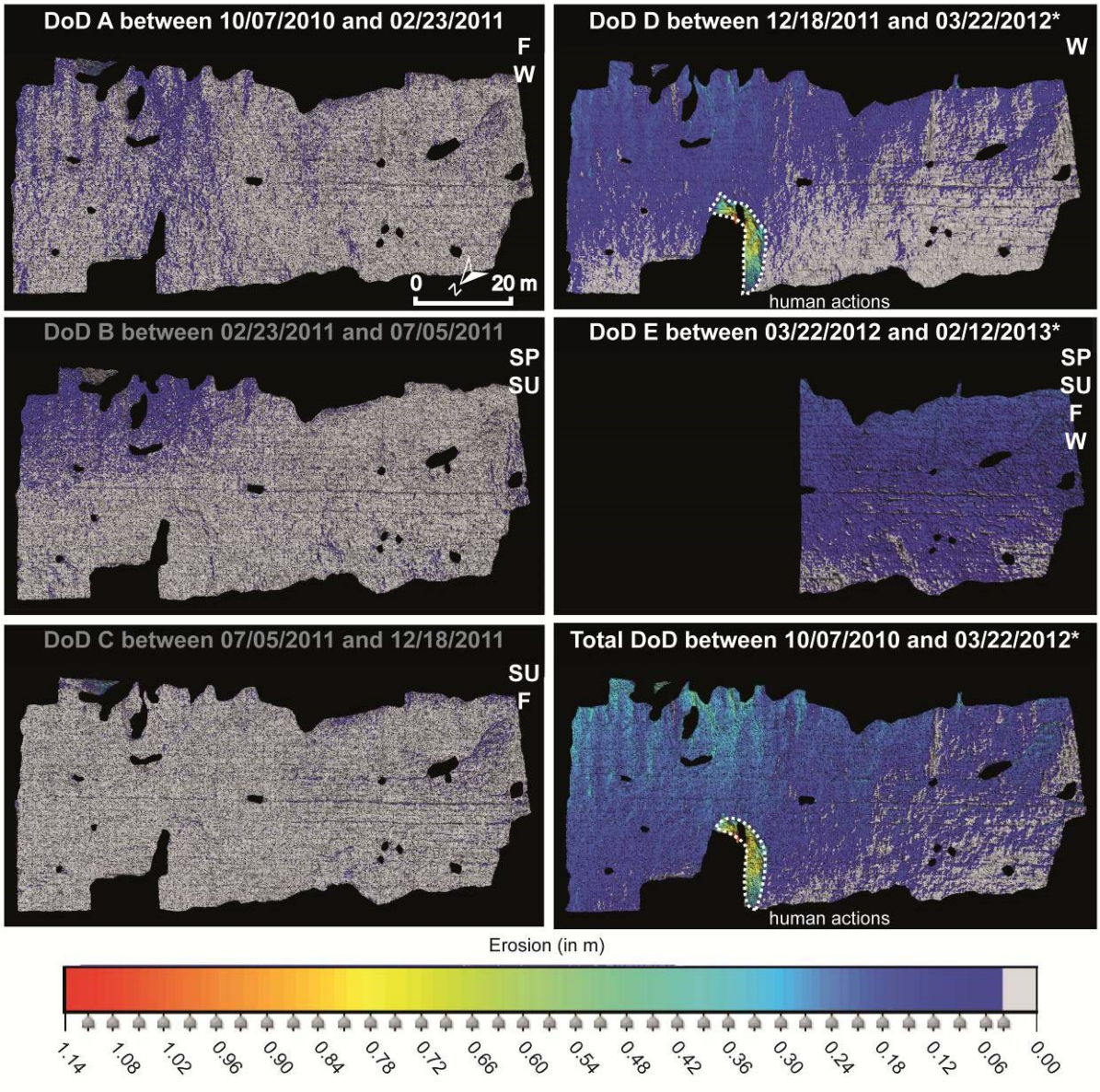

Fig. 6: DoDs of the cliff face at Dieppe 1 W between 10/07/2010 and 02/12/2013 (gray title: DoD affected by a high error margin; F: fall, W: winter, SP: spring, SU: summer; *: with human actions)

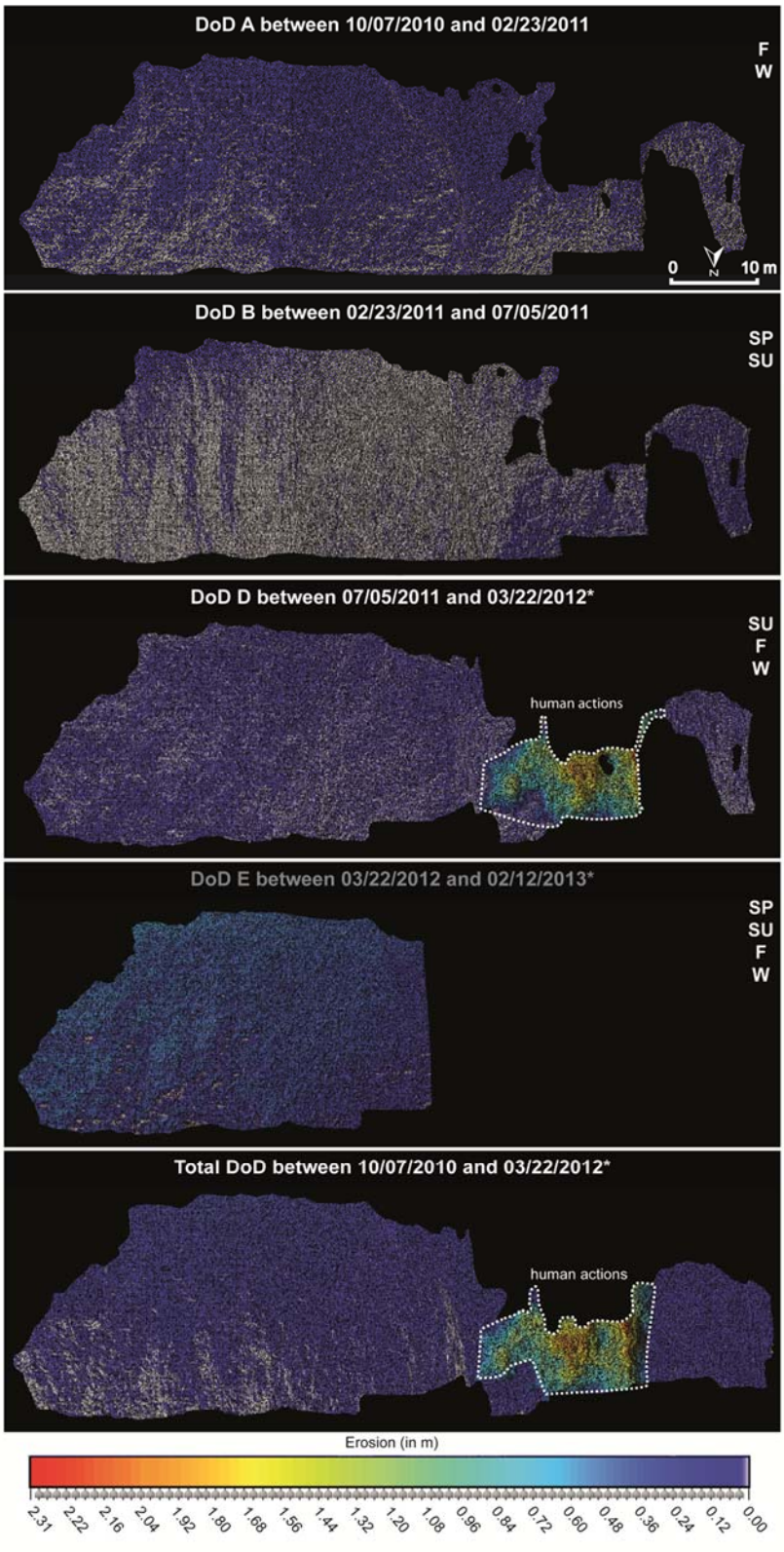

297

298 Fig. 7: DoDs of the cliff face at Dieppe 2 N between 10/07/2010 and 02/12/2013 (gray title:
299 DoD affected by a high error margin; F: fall, W: winter, SP: spring, SU: summer; *: with
300 human actions)

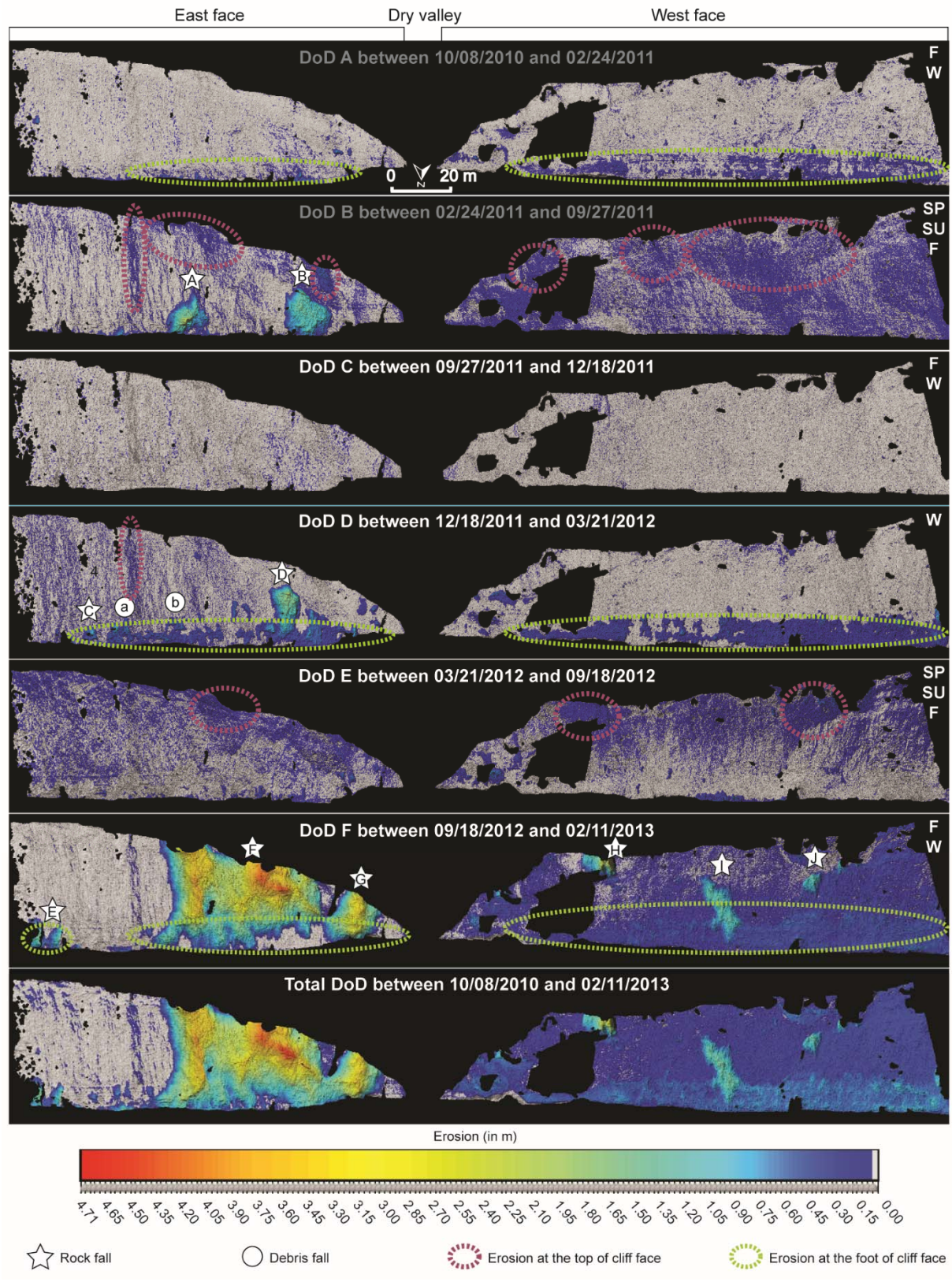

301

302 Fig. 8: DoDs of the cliff face at Petit Ailly between 10/08/2010 and 02/11/2013 (gray title:

303 DoD affected by a high error margin; F: fall, W: winter, SP: spring, SU: summer)

304 Thus, on the active cliff, debris falls represented 25% of the total retreat over the period
305 studied (Fig. 9). Debris falls are responsible for a retreat of 0.06 m y^{-1}, against 0.18 m y^{-1} for
306 rock falls over 28 months under a total retreat rate of 0.24 m y^{-1}. The rate related to debris
307 falls is consistent with the retreat rate for the abandoned cliffs (0.06–0.08 m y^{-1}) where only
308 debris falls were observed (Fig. 9).
309

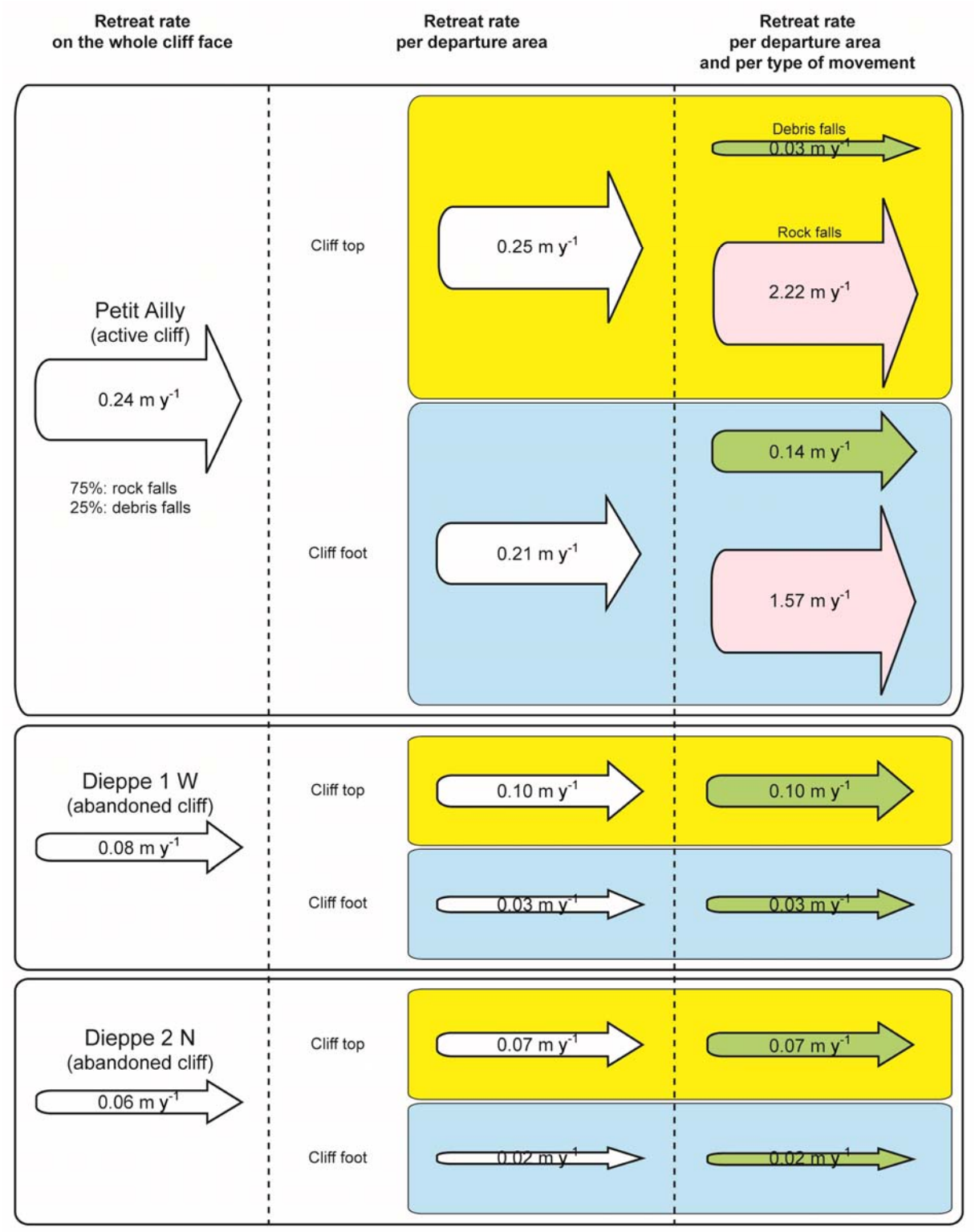

Fig. 9: Retreat rates as a function of departure area and type of movement

4.3. One of the modalities of cliff retreat highlighted

The DoD B in Fig. 8 shows departures of rocky material at the active cliff foot (east face). These departures occur by two rock falls, which have various depths. Rock fall A generates a maximal basal notch of 2.26 m (59 m^3) while rock fall B creates a maximal notch of 1.61 m (89 m^3). Later, in the DoD D (Fig. 8), debris fall b (0.61 m maximum deep, 2 m^3) and rock fall D (2.05 m maximum deep, 86 m^3) occur near these initial notches. Notches seem to propagate instability gradually at their periphery and often towards the top of the cliff. A few months later (DoD F), rock falls of the whole cliff face are observed at or next to these locations (rock falls F and G with a volume of 1,636 m^3 and 194 m^3, respectively). This study highlights one of the retreat modalities: the creation of a basal notch that, by overhanging, will gradually destabilize the top of the cliff to generate a rock fall of massive volume from the whole cliff face.

5. Discussion

Due to its centimeter precision and high temporal frequency, monitoring by TLS has provided a new understanding of the retreat of chalk cliff faces at the study sites. Some of the results generate discussion, which is organized in four points: 1) the spatial distribution of the retreat over the short and long terms; 2) the proportion of debris falls in retreat; 3) the modality of cliff retreat; and 4) the determination of possible agents and processes responsible for erosion.

Over 28 months of repeated surveys, the cliff top retreated faster than the cliff foot for both active and abandoned cliffs. At the abandoned cliff, this result seems to be a normal evolution because, since the polder construction in the early 1980s, the slope has evolved exclusively under subaerial agents. These agents are particularly efficient at the cliff top. Over a longer timescale, the retreat rates should not converge. The final result should be a terrestrial slope. In contrast, this situation may appear surprising at the active cliff of Petit Ailly. The foot of the active cliff should be more eroded due to a combination of marine and subaerial agents. This result can be explained by the lithology and the timescale of our study. This active cliff has a specific morphostructural context: the chalk has overlying Tertiary

342 strata. In these strata, there are water tables from where runoff may affect the chalk cliff top.
343 This process may create a temporarily high retreat of the chalk cliff top. Over a longer
344 timescale, the retreat difference between the foot and the top of the cliff should change.
345 Indeed, there is a "*disconnect in the timescale of our monitoring and the cliff morphology*"
346 (Rosser et al., 2013). On the active cliff, these two rates should evolve to fit with the sub-
347 vertical profile of the current cliff (Fig. 10). Otherwise, the form of the cliff should change.

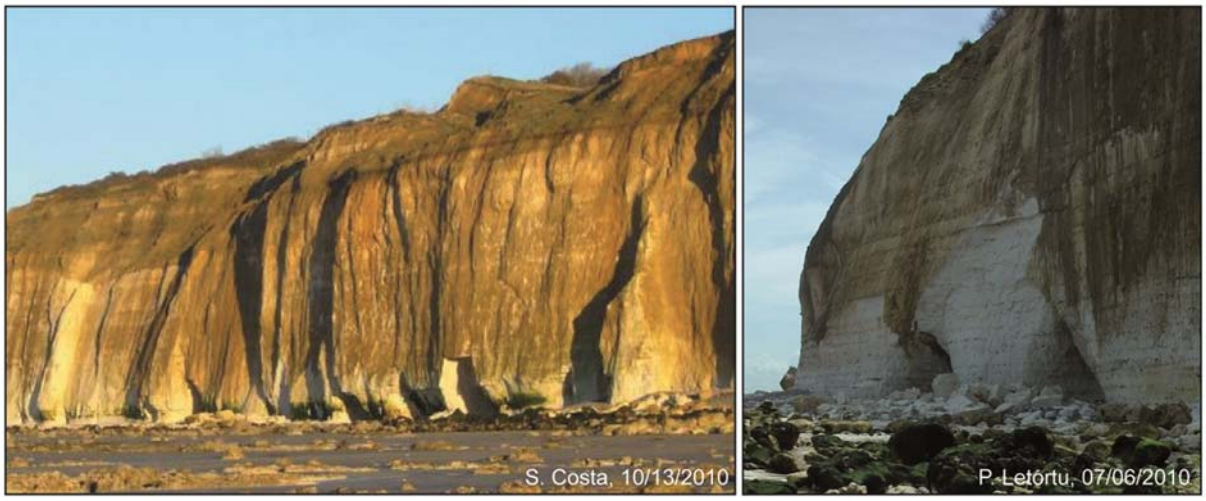

348

349 Fig. 10: Sub-vertical cliff profiles and basal notches in Sainte-Marguerite-sur-Mer (Cap
350 d'Ailly)

351

352 Our study also highlights that debris falls correspond to 25% of the total retreat of the active
353 cliff. They are responsible for a retreat rate of 0.06 m y^{-1}, while rock falls are responsible for a
354 retreat rate of 0.18 m y^{-1} during the 28 months. This share is much greater than those
355 reported by May and Heeps (1985) and Hénaff et al. (2002) (10% and 11%, respectively).
356 Nevertheless, as suggested by Costa (1997), this proportion of debris falls is highly variable
357 in time and may be quickly removed. Costa (1997) measured a retreat of 0.02 m for a single
358 event (a rapid thaw on 31 December 1995) along the same coastline. Fortunately, these
359 debris falls were observed but were removed at high tide. Our repeated surveys by TLS and
360 the resultant visualization of erosion in the centimeter scale better quantify these debris falls.
361 These surveys over 28 months also enable one of the modalities of cliff retreat to be
362 identified. On the east side of the dry valley at Petit Ailly, the upward propagation of failure

from a destabilizing notch at the cliff foot is observed. This recalls the usual scenario (sometimes considered simplistic) of a basal notch (Sunamura, 1988, 1992; Trenhaile, 1987; Stephenson et al., 2013; Trenhaile et al., 2013) leading to larger rock falls named overhanging movements (Hantz et al., 2003; Andriani and Walsh, 2007). Our work reveals, like Rosser et al. (2013) along the cliffs of the North York Moors National Park (UK), that departure areas evolve over time around their periphery with a dominant upward direction (vertical and subvertical). Thus, the authors stated that the distribution of rock falls may not be random: "*there is clear spatial clustering indicative of propagation when rock falls are considered as cumulative through time*". These notches (created by debris falls or rock falls) are visible in many places along the Upper Normandy coast (Costa, 1997), especially along Cap d'Ailly (Fig. 10). They may be a warning sign of more massive failure (the date is still difficult to predict) which can cover the whole cliff face (Young et al., 2009). As Terzaghi (1950) suggested, slow surface movements precede catastrophic landslides. He added, "*if a landslide comes as a surprise to the eyewitnesses, it would be more accurate to say that the observers failed to detect the phenomena which preceded the slide…*". Further investigations are needed to understand better the link between preparatory phenomena and rock falls. The combination of knowledge about the location, the time of cliff retreat, and the type of movement (debris falls and rock falls) may provide hypotheses about the agents (marine or subaerial) and processes responsible for erosion. Debris falls affect both sites (Dieppe and Petit Ailly) and are present on the whole cliff faces. A large production of debris falls was observed at the foot of the Petit Ailly active cliff (green circles in electronic version of Fig. 8). The location of erosion is specific: it occurs only at the first 10 m of the cliff face. This erosion is not found at the base of the abandoned cliffs in Dieppe. These features raise questions about the agents and processes responsible for erosion. This basal erosion of the active cliff may be induced by the water table, which saturates the chalk with water, prone to hydroclasty and cryoclasty. However, the abandoned cliffs where there is the water table and other subaerial agents should also have this basal erosion. Thus, marine actions may lead to basal erosion by debris falls. The first 10 m of erosion at the cliff foot are consistent with the

391 height of the waves that can reach it locally. Erosion due to marine actions may be quantified
392 by deduction. At the foot of the abandoned cliffs, the annual retreat rate related to debris
393 falls, and exclusively due to subaerial agents, is 0.03 m y^{-1}. Along the active cliff, the retreat
394 rate related to debris falls is 0.14 m y^{-1} (Fig. 9) but includes subaerial and marine agents.
395 Marine actions may be responsible for a retreat rate by debris falls of 0.11 m y^{-1} of the
396 observed 0.14 m y^{-1}. Thus, at the active cliff foot, marine actions may generate a retreat by
397 debris falls four times higher than subaerial actions. This simple (perhaps simplistic)
398 deduction may provide the first elements of quantification of marine actions. Again, marine
399 actions may be an efficient agent of erosion.
400 The marine actions may not be uniform at the active cliff foot (Fig. 8). The sides of the dry
401 valley evolve differently. The west face has higher debris fall retreat at the cliff foot than the
402 east face. This difference at fine scale may be due to the presence of a man-made structure,
403 a groin, located in the axis of the dry valley. Indeed, this structure leads to an accumulation
404 of gravels at the west face. As Robinson (1977) observed an increase in cliff erosion by a
405 factor of 18 when beach sediments were present compared to when they were not, we
406 suggest these gravels may be used as projectiles by the swell and may explain the high
407 abrasion by debris falls at the cliff foot on the west face (Fig. 11). On the east face, waves
408 breaking without projectiles may be less effective. These observations converge towards
409 model results (Sunamura, 1982, 1992; Limber and Murray, 2011; Kline et al., 2014).
410 Sunamura (1982, 1992) showed in laboratory experiments that cliffs and beaches exhibit
411 internal feedbacks. The amount and configuration of beach material can bring positive
412 feedback with higher wave erosive efficacy by providing abrasive agents (Sunamura, 1992).
413 Kline et al. (2014) studied the role of mechanical abrasion by beach sediments in
414 cliff/platform/beach evolution over a long timescale (up to 1,000 years). They suggest that
415 "*mechanical abrasion is a feasible mechanism of cliff and platform evolution".* However, on
416 the whole cliff face scale at Petit Ailly, the east face has a higher retreat rate than the west
417 face (0.39 m y^{-1} against 0.12 m y^{-1}). This is due to numerous rock falls that occur on the east
418 face but rarely on the west face. Dewez et al. (2013) also observed rock falls at the cliff foot

419 at the downdrift side of the groin of Criel-sur-Mer (20 km north of Dieppe). They mentioned
420 the caving effect of waves by hydraulic forces including water hammer and air compression,
421 particularly effective without a beach (gravel transit is blocked by the 120 m-long groin). At
422 the Petit Ailly, this effect is possible due to the lack of beach on the downdrift side of the
423 groin. There is no protecting gravel beach. When a rock fall occurs, most fallen rocks are
424 quickly removed. Therefore, water hammer and air compression may be more intense and
425 may generate rock falls. This suggestion underlines the role of marine actions as an erosion
426 agent and the dual role of a gravel beach, which can protect the cliff foot or attack it (Costa et
427 al., 2006b). Future TLS surveys here will be valuable to provide complementary information
428 over a longer timescale, leading to a better understanding of the roles of marine actions and
429 gravel beaches.
430

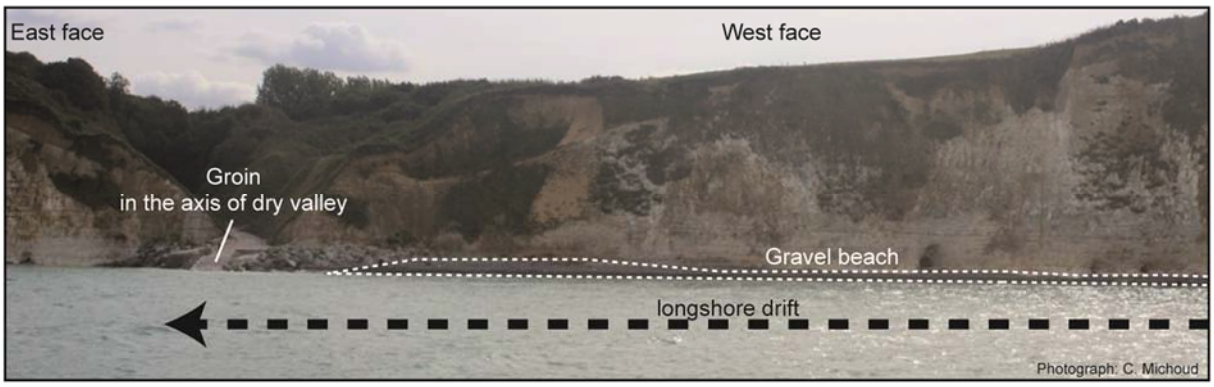

431
432 Fig. 11: Mid-tide (coefficient 106) at Petit Ailly and position of gravel beach
433
434 The departure of debris falls at the active cliff top, and sometimes reaching the mid-cliff, is
435 visible on the DoDs B and E (purple circles in electronic version of Fig. 8) during off-winter
436 periods, thus without frost. In the context of an abandoned cliff, the location of debris falls
437 also highlights linear shapes (Figs. 6 and 7). The often linear shapes of the departure areas
438 and their concentration in dihedrons seem to be runoff zones, and thus subaerial actions.
439 Subaerial actions may not be negligible in the context of an active cliff.
440 In this paper, erosion agents have been discussed – marine actions with mechanical
441 abrasion, water hammer, air compression, and subaerial agents with runoff. These

hypotheses open up research perspectives about the quantification of their action. Beyond increasing the temporal representativeness of monitoring, reducing the time interval between each survey and conducting surveys before/during/after specific weather and sea conditions including freeze/thaw cycles and storms, supplementary measurements will be carried out to 1) monitor the behavior of water tables that could affect the stability of the cliff; 2) obtain a fine acquisition of rainfall, thermal and swell data; and 3) quantify the role of marine actions in the destabilization of the chalk massif.

It is necessary to focus not only on the external agents of erosion but also on internal factors such as chalk fracturing, which alters material resistance and often predetermines the extent of rock falls. To deal with the problem of spatial representativeness and check if our results are replicable, other lithologies of cliff faces are currently under study.

6. Conclusions

In Upper Normandy, the repeated surveys over 28 months on two sites with similar lithostratigraphic characteristics but different exposures to marine actions, highlight that cliff retreat is highly variable in time, location, its modalities, and the agents/processes involved. The active cliff of Petit Ailly (Varengeville-sur-Mer) has regressive dynamics 3–4 times greater than the abandoned cliffs of Dieppe (0.24 m y^{-1} against 0.06–0.08 m y^{-1}). This difference highlights the importance of marine actions in erosion dynamics. Whereas the abandoned cliff recedes only with debris falls, the active cliff has a combination of debris falls (25% of the retreat) and rock falls (75%). On both sites, a spatial variation in retreat rates can be observed over this short timescale: the cliff top recedes faster than the cliff foot. Moreover, due to the fine location of the retreat obtained by our methodology, one of the modalities of retreat is detected. Precursory movements creating a basal notch later generate massive rock falls on the whole cliff face. These results indicate that TLS can be very useful for the spatial prediction of rock falls and for contributing to the debate about the agents and processes responsible for erosion.

Acknowledgements

We thank the reviewers for their detailed reviews of the manuscript and their helpful comments.

References

Abellán, A., Jaboyedoff, M., Oppikofer, T., Vilaplana, J.M., 2009. Detection of millimetric deformation using a terrestrial laser scanner: experiment and application to a rock fall event. Natural Hazard and Earth System Sciences 9(2), 365-372.

Abellán, A., Calvet, J., Vilaplana, J.M., Blanchard, J., 2010. Detection and spatial prediction of rock falls by means of terrestrial laser scanner monitoring. Geomorphology 119(3), 162-171.

Abellán, A., Oppikofer, T., Jaboyedoff, M., Rosser, N.J., Lim, M., Lato, M.J., 2014. Terrestrial laser scanning of rock slope instabilities. Earth Surface Processes and Landforms 39(1), 80-97.

Andriani, G.F., Walsh, N., 2007. Rocky coast geomorphology and erosional processes: A case study along the Murgia coastline South of Bari, Apulia - SE Italy. Geomorphology 87(3), 224-238.

Bignot, G., 1962. Étude sédimentologique et micropaléontologique de l'Éocène du Cap d'Ailly (près de Dieppe, Seine-Maritime). Ph.D. Thesis, University of Paris, France.

Bird, E., 2008. Coastal Geomorphology. An introduction (Second Edition). Wiley, New York.

Costa, S., 1997. Dynamique littorale et risques naturels: L'impact des aménagements, des variations du niveau marin et des modifications climatiques entre la baie de Seine et la baie de Somme. Ph.D. Thesis, University of Paris I, France.

Costa, S., Delahaye, D., Freiré-Diaz, S., Di Nocera, L., Davidson, R., Plessis, E., 2004. Quantification of the Normandy and Picardy chalk cliff retreat by photogrammetric analysis. In: Mortimore, R.N., Duperret, A. (Eds.), Coastal chalk cliff instability. Engineering Geology Special Publications, London, pp. 139-148.

Costa, S., Laignel, B., Hauchard, E., Delahaye, D., 2006a. Facteurs de répartition des entonnoirs de dissolution dans les craies du littoral du Nord-Ouest du Bassin de Paris. Zeitschrift für Geomorphologie 50, 95-116.

Costa, S., Hénaff, A., Lageat, Y., 2006b. The gravel beaches of north-west France and their contribution to the dynamic of the coastal cliff-shore platform system. Zeitschrift für Geomorphologie, Suppl.-Vol 144, 199-214.

Delacourt, C., Allemand, P., Berthier, E., Raucoules, D., Casson, B., Grandjean, P., Pambrun, C., Varel, E., 2007. Remote-sensing techniques for analysing landslide kinematics: a review. Bulletin de la Société Géologique de France 178(2), 89-100.

Dewez, T.J.B., Rohmer, J., Regard, V., Cnudde, C., 2013. Probabilistic coastal cliff collapse hazard from repeated terrestrial laser surveys: case study from Mesnil Val (Normandy, northern France). Journal of Coastal Research, Special Issue 65, 702-707.

Griggs, G.B., Trenhaile, A.S., 1994. Coastal cliff and platform. In: Carter, R.W.G., Woodroffe, C.D. (Eds.), Coastal Evolution. Cambridge Univ. Press, Cambridge, pp. 425-450.

Hantz, D., Vengeon, J.M., Dussauge-Peisser, C., 2003. An historical, geomechanical and probabilistic approach to rock-fall hazard assessment. Natural Hazards and Earth System Sciences 3(6), 693-701.

Hénaff, A., Lageat, Y., Costa, S., Plessis, E., 2002. Le recul des falaises crayeuses du Pays de Caux: détermination des processus d'érosion et quantification des rythmes d'évolution. Géomorphologie: Relief, Processus, Environnement 8(2), 107-118.

Jaud, M., 2011. Techniques d'observation et de mesure haute résolution des transferts sédimentaires dans la frange littorale. Ph.D. Thesis, University of Bretagne Occidentale, France.

Juignet, P., Breton, G., 1992. Mid-Cretaceous sequence stratigraphy and sedimentary cyclicity in the western Paris Basin. Palaeogeography, Palaeoclimatology, Palaeoecology 91(3), 197-218.

Kline, S.W., Adams, P.N., Limber, P.W., 2014. The unsteady nature of sea cliff retreat due to mechanical abrasion, failure and comminution feedbacks. Geomorphology 219, 53-67.

525 Kuhn, D., Prüfer, S., 2014. Coastal cliff monitoring and analysis of mass wasting processes
526 with the application of terrestrial laser scanning: A case study of Rügen, Germany.
527 Geomorphology 213, 153-165.
528 Laignel, B., 1997. Les altérites à silex de l'ouest du Bassin de Paris: caractérisation
529 lithologique, genèse et utilisation potentielle comme granulats. Ph.D. Thesis, University of
530 Rouen, France.
531 Lasseur, E., 2007. La Craie du Bassin de Paris (Cénomanien-Campanien, Crétacé
532 supérieur). Sédimentologie de faciès, stratigraphie séquentielle et géométrie 3D. Ph.D.
533 Thesis, University of Rennes 1, France.
534 Lautridou, J.P., 1985. Le cycle périglaciaire pléistocène en Europe du Nord-Ouest et plus
535 particulièrement en Normandie. Ph.D. Thesis, University of Caen Basse-Normandie, France.
536 Letortu, P., 2013. Le recul des falaises crayeuses haut-normandes et les inondations par la
537 mer en Manche centrale et orientale: de la quantification de l'aléa à la caractérisation des
538 risques induits. Ph.D. Thesis, University of Caen Basse-Normandie, France.
539 https://halshs.archives-ouvertes.fr/file/index/docid/1018719/filename/These_Letortu.pdf
540 Letortu, P., Costa, S., Bensaid, A., Cador, J.M., Quénol, H., 2014. Vitesses et rythmes de
541 recul des falaises crayeuses de Haute-Normandie (France): méthodologie et variabilité du
542 recul. Géomorphologie, Relief, Processus et Environnement 2, 133-144.
543 Letortu, P., Costa, S., Cador, J.M., Coinaud, C., in press. Statistical and empirical analyses
544 of the triggers of coastal chalk cliff failure. Earth Surface Processes and Landforms.
545 Lichti, D.D., 2007. Error modelling, calibration and analysis of an AM-CW terrestrial laser
546 scanner system. ISPRS Journal of Photogrammetry and Remote Sensing 61(5), 307-324.
547 Lim, N., Petley, D.N., Rosser, N.J., Allison, R.J., Long, A.J., Pybus, D., 2005. Combined
548 digital photogrammetry and time-of-flight laser scanning for monitoring cliff evolution. The
549 Photogrammetric Record 20(110), 109-129.
550 Lim, M., Rosser, N.J., Allison, R.J., Petley, D.N., 2010. Erosional processes in the hard rock
551 coastal cliffs at Staithes, North Yorkshire. Geomorphology 114(1), 12-21.

552 Limber, P.W., Murray, A.B., 2011. Beach and sea-cliff dynamics as a driver of long-term
553 rocky coastline evolution and stability. Geology 39(12), 1147-1150.
554 May, V., Heeps, C., 1985. The nature and rates of changes on chalk coastlines. Zeitschrift
555 für Geomorphologie, Suppl.-Vol 57, 81-94.
556 Michoud, C., Carrea, D., Costa, S., Derron, M.H., Jaboyedoff, M., Davidson, R., Delacourt,
557 C., Letortu, P., Maquaire, O., 2014. Landslide detection and monitoring capability of boat-
558 based mobile laser scanning along Dieppe coastal cliffs, Normandy. Landslides, 1-16. DOI
559 10.1007/s10346-014-0542-5.
560 Mortimore, R.N., Duperret, A., 2004. Coastal chalk cliff instability. Engineering Geology
561 Special Publications, London.
562 Oppikofer, T., Jaboyedoff, M., Keusen, H.R., 2008. Collapse at the eastern Eiger flank in the
563 Swiss Alps. Nature Geoscience 1(8), 531-535.
564 Oppikofer, T., Jaboyedoff, M., Blikra, L., Derron, M.H., Metzger, R., 2009. Characterization
565 and monitoring of the Åknes rockslide using terrestrial laser scanning. Natural Hazards and
566 Earth System Sciences 9(3), 1003-1019.
567 Oppikofer, T., Bunkholt, H., Fischer, L., Saintot, A., Hermanns, R.L., Carrea, D., Longchamp,
568 C., Derron, M.H., Michoud, C., Jaboyedoff, M., 2012. Investigation and monitoring of rock
569 slope instabilities in Norway by terrestrial laser scanning. Proc. of the 11th International & 2nd
570 North American Symposium on Landslides, Banff, Canada, pp. 3-8.
571 Pomerol, B., Bailey, H.W., Monciardini, C., Mortimore, R.N., 1987. Lithostratigraphy and
572 biostratigraphy of the Lewes and Seaford chalks: a link across the Anglo-Paris basin at the
573 Turonian-Senonian boundary. Cretaceous Research 8(4), 289-304.
574 Quinn, J.D., Rosser, N.J., Murphy, W., Lawrence, J.A., 2010. Identifying the behavioural
575 characteristics of clay cliffs using intensive monitoring and geotechnical numerical modeling.
576 Geomorphology 120(3), 107-122.
577 RIEGL, 2007. Documentation technique du TLS (LMS-Z390i).
578 Robinson, L.A., 1977. Marine erosive processes at the cliff foot. Marine Geology 23(3), 257-
579 271.

580 Rodet, J., 1991. Les karsts de la craie: étude comparative. Ph.D. Thesis, University of Paris,
581 France.
582 Rosser, N.J., Petley, D.N., Lim, M., Dunning, S.A., Allison, R.J., 2005. Terrestrial laser
583 scanning for monitoring the process of hard rock coastal cliff erosion. Quarterly Journal of
584 Engineering Geology and Hydrogeology 38(4), 363-375.
585 Rosser, N.J., Lim, M., Petley, D.N., Dunning, S.A., Allison, R.J., 2007. Patterns of precursory
586 rockfall prior to slope failure. Journal of Geophysical Research: Earth Surface 112(F4).
587 Rosser, N.J., Brain, M.J., Petley, D.N., Lim, M., Norman, E.C., 2013. Coastline retreat via
588 progressive failure of rocky coastal cliffs. Geology 41(8), 939-942.
589 Rothmund, S., Niethammer, U., Malet, J.P., Joswig, M., 2013. Landslide surface monitoring
590 based on UAV- and ground-based images and terrestrial laser scanning: accuracy analysis
591 and morphological interpretation. First Break 31(8).
592 Rowlands, K.A., Jones, L.D., Whitworth, M., 2003. Landslide laser scanning: a new look at
593 an old problem. Quarterly Journal of Engineering Geology and Hydrogeology 36(2), 155-157.
594 Royán, M.J., Abellán, A., Jaboyedoff, M., Vilaplana, J.M., Calvet, J., 2014. Spatio-temporal
595 analysis of rock fall pre-failure deformation using Terrestrial LiDAR. Landslides 11(4), 697-
596 709.
597 Stephenson, W.J., Dickson, M.E., Trenhaile, A.S., 2013. Rock Coasts. In: Shroder, J.F.
598 (Ed.), Treatise on Geomorphology. Academic Press, San Diego, pp. 289-307.
599 Sturzenegger, M., Stead, D., 2009. Quantifying discontinuity orientation and persistence on
600 high mountain rock slopes and large landslides using terrestrial remote sensing techniques.
601 Natural Hazards and Earth Systems Science 9(2), 267-287.
602 Sunamura, T., 1982. A wave tank experiment on the erosional mechanism at a cliff base.
603 Earth Surface Processes and Landforms 7(4), 333-343.
604 Sunamura, T., 1988. Beach morphologies and their change. In: Horikawa, K. (Ed.),
605 Nearshore dynamics and coastal processes. University of Tokyo Press, Tokyo, pp. 136-161.
606 Sunamura, T., 1992. Geomorphology of Rocky Coasts. John Wiley & Son, London.

607 Terzaghi, K., 1950. Mechanism of landslides. In: Paige, S. (Ed.), Application of Geology to
608 Engineering Practice (Berkeley Volume). Geological Society of America, Washington, pp. 82-
609 123.
610 Teza, G., Galgaro, A., Zaltron, N., Genevois, R., 2007. Terrestrial laser scanner to detect
611 landslide displacement fields: a new approach. International Journal of Remote Sensing
612 28(16), 3425-3446.
613 Teza, G., Pesci, A., Genevois, R., Galgaro, A., 2008. Characterization of landslide ground
614 surface kinematics from terrestrial laser scanning and strain field computation.
615 Geomorphology 97(3), 424-437.
616 Travelletti, J., Oppikofer, T., Delacourt, C., Malet, J.P., Jaboyedoff, M., 2008. Monitoring
617 landslide displacements during a controlled rain experiment using a long-range terrestrial
618 laser scanning (TLS). International Archives of the Photogrammetry, Remote Sensing and
619 Spatial Information Sciences 37(B5), 485-490.
620 Travelletti, J., Delacourt, C., Malet, J.P., Allemand, P., Schmittbuhl, J., Toussaint, R., 2013.
621 Performance of Image Correlation Techniques for Landslide Displacement Monitoring. In:
622 Margottini, C., Canuti, P., Sassa, K. (Eds.), Landslide Science and Practice. Springer, Berlin
623 Heidelberg, pp. 217-226.
624 Trenhaile, A.S., 1987. The geomorphology of rock coasts. Oxford University Press, Oxford.
625 Trenhaile, A.S., Prestanski, K.J., Porter, N.I., Gagnon, J., 2013. Rock coast erosional forms
626 (notches and shore platforms) on the La Paz Peninsula, Southern Baja, Mexico. Geo-Temas
627 14, 1-4.
628 Varnes, D.J., 1978. Slope movement types and processes. In: Schuster, R.L., Krizek, R.J.
629 (Eds.), Landslides: Analysis and Control. Transportation and Road Research Board, National
630 Academy of Science, Washington, pp. 11-33.
631 Young, A.P., Flick, R.E., Gutierrez, R., Guza, R.T., 2009. Comparison of short-term seacliff
632 retreat measurement methods in Del Mar, California. Geomorphology 112(3), 318-323.